

Please cite this article as: Z. Zhong, E. E.Lee, M. Nejad and J. Lee, "Influence of CAV clustering strategies on mixed traffic flow characteristics: an analysis of vehicle trajectory data," *Transp. Res. Part C: Emerging Technologies*, vol.115, pp.102611, 2020, doi:10.1016/j.trc.2020.102611

Influence of CAV Clustering Strategies on Mixed Traffic Flow Characteristics: An Analysis of Vehicle Trajectory Data

Zijia Zhong^{a,*}, Earl E. Lee^a, Mark Nejad^a, Joyoung Lee^b

^a*Department of Civil and Environmental Engineering, University of Delaware, United States*

^b*John A. Reif, Jr. Department of Civil and Environmental Engineering, New Jersey Institute of Technology, United States*

Abstract

Being one of the most promising applications enabled by connected and automated vehicles (CAV) technology, Cooperative Adaptive Cruise Control (CACC) is expected to be deployed in the near term on public roads. Thus far, the majority of the CACC studies have been focusing on the overall network performance with limited insights on the potential impacts of CAVs on human-driven vehicles (HVs). This paper aims to quantify such impacts by studying the high-resolution vehicle trajectory data that are obtained from microscopic simulation. Two platoon clustering strategies for CACC- an ad hoc coordination strategy and a local coordination strategy-are implemented. Results show that the local coordination outperforms the ad hoc coordination across all tested market penetration rates (MPRs) in terms of network throughput and productivity. According to the two-sample Kolmogorov-Smirnov test, however, the distributions of the hard braking events (as a potential safety impact) for HVs change significantly under local coordination strategy. For both of the clustering strategy, CAVs increase the average lane change frequency for HVs. The break-even point for average lane change frequency between the two strategies is observed at 30% MPR, which decreases from 5.42 to 5.38 per vehicle. The average lane change frequency following a monotonically increasing pattern in response to MPR, and it reaches the highest 5.48 per vehicle at 40% MPR. Lastly, the interaction state of the car-following model for HVs is analyzed. It is revealed that the composition of the interaction state could be influenced by CAVs as well. One of the apparent trends is that the time spent on approaching state declines with the increasing presence of CAVs.

Keywords: Platoon Formation, Cooperative Adaptive Cruise Control, Vehicle Trajectory Analysis, Mixed Traffic Conditions, CACC Degradation, Human Factor

1. Introduction

Cooperative adaptive cruise control (CACC) enables closely-coupled vehicular platoons by extra layers of communication and automation. Being one of the most-studied applications of the connected and automated vehicle (CAV) technology, CACC is expected to drastically increase mobility and decrease emissions, while providing a safer and more convenient way for vehicle occupants. Studying CACC under mixed traffic conditions in anticipation of its near-term deployment has gained a significant amount of attention ([Amirgholy](#)

*Corresponding author: Zijia Zhong. The research was conducted at the University of Delaware; the author is now with the Center for Integrated Mobility Sciences at the National Renewable Energy Laboratory.

Email addresses: zijia.zhong@nrel.gov (Zijia Zhong), elee@udel.edu (Earl E. Lee), nejad@udel.edu (Mark Nejad), jo.y.lee@njit.edu (Joyoung Lee)

et al., 2020; Ghiasi et al., 2019; Saha et al., 2019; Wang et al., 2019a; Zhao et al., 2018). The near-term deployment of CACC likely entails the following conditions: i) relatively low CACC market penetration (e.g., less than 40%), ii) the substantial presence of non-equipped vehicle without communication capability (i.e., human-driven vehicles (HVs)), iii) legacy roadway infrastructure that is not optimized for CACC operation (e.g., mixed-use travel lane, lack of roadside units). Local coordination allows CAV vehicles within a certain distance to form a string of CAVs (or vehicular platoon). Such a strategy is appealing to minimize CACC degradation (Wang et al., 2019a), where a CAV operates under ACC mode.

Thus far, the CACC evaluation has been focusing on the benefits that CAV could potentially bring to the transportation networks. However, the potential impacts of platoon clustering strategies on non-equipped vehicles (i.e., HVs) have been seldom studied. Empirical trajectory data revealed that lane change caused by merging and diverging vehicle creates most motorway turbulence (van Beinum et al., 2018). Therefore, CACC may influence the characteristics of the HV flow when a local coordination strategy is employed. More specifically, the expected potential impacts of CACC systems on HVs may include: i) additional weaving during CACC clustering, ii) lane changes by HVs induced by the aforementioned CACC clustering, iii) increase collision risks, and iv) lane blockages by CACC platoons.

In this study, the traffic flow characteristics of the HVs, instead of the CAVs, are examined when ad hoc coordination and local coordination strategies for CACC is deployed. The interactions between HVs and CAVs are analyzed based on the high-resolution vehicle trajectory data that are extracted from microscopic simulations. The interaction state among HVs is also studied to derive insights. The proposed method is also suitable for extracting the driving behavioral data for future field deployment and modeling heterogeneous traffic flow that is consisted of HVs and CAVs.

The organization of the remainder of the paper is as follows. Relevant literature regarding studies of CACC in mixed traffic is reviewed in Section 2, followed by the evaluation method in Section 3. The simulation results are discussed in Section 4. Lastly, findings and recommendations are presented in Section 5.

2. Relevant Research

CACC can positively improve traffic performance with a sufficient presence, which is commonly expressed as the market penetration rate (MPR). MPR is the ratio of a product or service that is being used by customers and the total estimated demand. As the CACC technology advances, we have seen an increasing amount of field experiments for CACC (Aarts and Feddes, 2016; Chang et al., 2018; Ma et al., 2019; Milanés and Shladover, 2014; Xu and Peng, 2019). However, the majority of them have a limited scale and focus on the hardware aspect of the vehicle. It is difficult to extrapolate the testing results at the traffic flow level. Thus far, analytical and simulation approaches remain the two primary methods for evaluating the traffic impact of CACC. Analytical approaches mainly based on the macroscopic traffic flow model. It may not faithfully capture the nonlinear phenomena in traffic flow (e.g., lane drop), and it only identifies the impact of a limited number of factors. In comparison, microscopic traffic simulation is capable of capturing more complex traffic phenomena and has been widely adopted.

The effectiveness of CACC depends on three major factors: i) achievable headway, ii) car-following model, and iii) market penetration rate (MPR). The reduced time headway and following distance have been recognized as primary benefits of CACC. CACC string can operate with an 0.6 s intra-platoon headway, compared to the 1.4 s or longer time gap for humans (Nowakowski et al., 2010). Some CACC studies aimed to estimate the achievable roadway capacity with simple network topology (e.g., single-lane freeway). Van Arem et al. (2006) assessed the impact of CACC on freeway traffic flow on a 6-km, one-lane freeway with ramps distributed with a 1.6-km interval. They found the roadway capacity reached 4,250 vehicles per hour (vph) per lane with full CACC penetration. Using the same CACC model, Shladover et al. (2012) found the lane capacity of 3,600 vph at 90% MPR on a one-lane freeway. Talebpour and Mahmassani (2016) proposed an analytical framework for modeling the longitudinal interaction among regular, connected, and autonomous vehicles with the focus on investigating the string stability of the heterogeneous flow. The simulation was conducted on a hypothetical one-lane highway, and mixed traffic flow performance was measured at an aggregated level. However, the single-lane freeway cases are prone to overestimate the mobility benefits

brought by CACC by excluding lateral interaction or lane changing among the multi-lane segment on the mainline. Hence evaluation of multi-lane scenarios provide more realistic estimation, and they can be found in [Arnaout and Arnaout \(2014\)](#); [Lee et al. \(2014\)](#); [Songchitruksa et al. \(2016\)](#)

The heterogeneous traffic flow attributed to partial market penetration has been examined in recent years. [Wang et al. \(2017a\)](#) proposed a second-order traffic flow model for mixed traffic streams with HVs and AVs. [Xiao et al. \(2018\)](#) studied the traffic flow characteristics using a multi-regime car-following model that is capable of switching among human-driven, ACC, and CACC modes. The Lane Change Model with Relaxation and Synchronization ([Schakel et al., 2012](#)) was adopted by Xiao et al., but no clustering strategy for CACC was implemented in the study conducted. In mixed traffic flow, the degradation of CACC occurs when a CACC vehicle follows a non-equipped vehicle that does not has communication capability. Under this circumstance, a CACC vehicle reverts to traditional ACC mode with a more conservative target headway. The negative effect of ACC on the system capacity is due to the higher time gap of ACC ([S. C. Calvert and van Lint, 2017](#)). [Wang et al. \(2019a\)](#) investigated the degradation of CACC in mixed traffic and the resulting flow stability. They found that the degraded CACC vehicles, based on current technical maturity, contributed negatively to the stability of the heterogeneous flow.

Insofar, the studies on the CACC impact on HVs are relatively scarce in the literature. The majority of the CACC study for human factors pertains to the human-machine interface, especially for the transition of authority at a low or medium level of automation ([Berghöfer et al., 2018](#); [Lank et al., 2011](#); [Naujoks et al., 2017](#); [Shen and Neyens, 2017](#)). [Nowakowski et al. \(2010, 2011\)](#) studied the acceptance of the short following time headway (ranging from 0.6 s to 1.1 s) enabled by CACC. As discovered, while all the drivers showed the willingness to accept the shorter following gaps, male participants were more likely to choose a shorter following distance. The carry-over effect of the short headway in manual driving was exhibited even after the disengagement from the platoons in the KONVOI project ([Casey and Lund, 1992](#)). [Gouy et al. \(2014\)](#) investigated the behavioral adaptation effects that potentially caused by the short headway of CACC platoon using driving simulators. Participants were instructed to drive alongside two CACC platoon configurations: i) a 10-truck platoon with 0.3-s intra-platoon headway, and ii) a 3-truck platoon with 1.4-s intra-platoon headway. A smaller average time headway was observed when in the short headway scenario. In the first platoon scenarios, participants spent more time under a 1-s headway, which is deemed unsafe ([Fairclough et al., 1997](#)).

The safety of the heterogeneous flow has been studied as well. [Papadoulis et al. \(2019\)](#) assessed the safety benefit of CAV and found 12-47% reduction in traffic conflict at 25% MPR. Local coordination among CAV was implemented with a threshold of 0.6 s from the vehicle upstream and downstream in the target lane. The safety implication of the driving aggressiveness of AV for the mixed traffic condition was studied by [Lee et al. \(2019\)](#). The conflict rate, which is derived from the vehicle interactions between AV and HV at each simulation time step, was used as a safety indicator among nine levels of CAV aggressiveness. However, the performance of each vehicle group was not separated, and the efficacy of simulating AV behavior by merely adjusting the Wiedemann model is still subject to debate ([Milanés and Shladover, 2014](#)).

In anticipation of the long lead-time for full market penetration, operation strategies of CACC in mixed traffic conditions have also been actively investigated. Managed lane, vehicle awareness device (VAD), and local coordination are among the most popular operation strategies. The underlying goal of these three methods is to alleviate the CACC degradation. Managed lane has a track record in incentivizing desired travel patterns or behaviors ([Shewmake and Jarvis, 2014](#)). [Liu et al. \(2018\)](#) presented a modeling framework for mixed traffic under various CACC operation strategies. The study revealed the quadratic relationship between pipeline capacity and MPR. Providing priority or exclusive access for CACC to managed lane could create concentrated segments of CACC vehicles, hence mitigating the degradation effects as demonstrated in previous studies ([Ghiasi et al., 2017](#); [Hussain et al., 2016](#); [Liu et al., 2018](#); [Qom et al., 2016](#); [Zhang et al., 2018](#); [Zhong and Lee, 2019](#)).

A vehicle awareness device (VAD) is the communication device that enables a HV to transmit real-time information to the surrounding CACC vehicles. Studies found that VADs can reduce CACC degradation by enabling quicker reactions of CACC vehicles ([Liu et al., 2018](#); [Shladover et al., 2012](#)), and it has emerged as one of the most promising strategies. The third operation strategy, which is of high relevance in this study, is the CACC coordination. As illustrated in Fig. 1, there are three types of clustering strategies: ad

hoc (AH) coordination, local coordination (LC), and global coordination (Shladover et al., 2012). In this study, only the former two clustering strategies are evaluated. The global coordination requires advance planning for the travel demand at the origin-designation level. CAVs are coordinated to enter the highway in platoons. Therefore, the impacts of global coordination probably concentrate at the merging area in the vicinity of the on-ramps, which does not fall within the scope of this study.

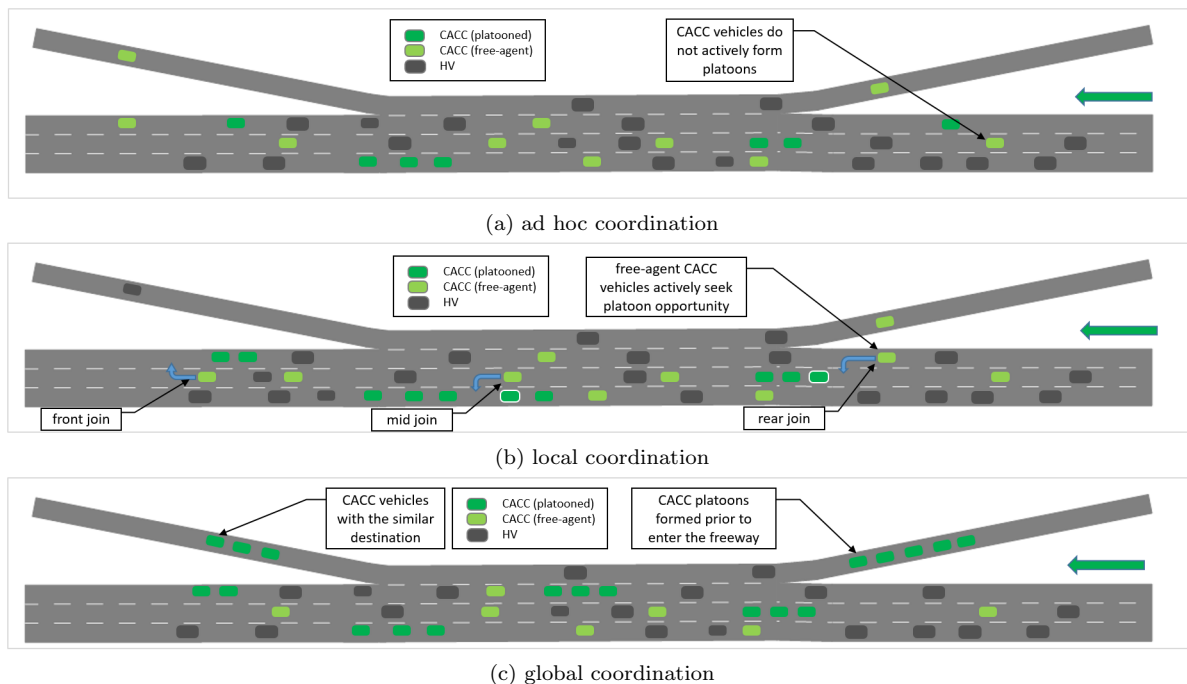


Fig. 1: CACC clustering strategy

Ad hoc coordination assumes random arrival of CAVs and no coordination among them. Therefore, the probability of driving behind another CAV is highly correlated to MPR. Ad hoc coordination has been observed in the majority of the research due to its simplicity in implementation and the lack of the conceptual framework for CAV platoon formation. However, the ad hoc coordination is not likely to harness the full potential of CACC, as it does not fully utilize the short intra-platoon headway enabled by the CAV technology. Exclusive lane, or other forms of the managed lane, has been employed to aid the ad hoc coordination (Segata et al., 2012).

Local coordination facilitates platoon formations, where free-agent CAVs are actively seeking clustering opportunities in their surroundings. It has been demonstrated in several notable field experiments, such as SATRE (Chan, 2016), COMPANION (Eilers et al., 2015). The subject CAV, as well as the surrounding CAVs, can be coordinated to change their trajectories to facilitate clustering. There are four basic types of lane change: i) free-agent-to-free-agent lane change, ii) free-agent-to-platoon lane change, iii) platoon-to-free-agent lane change, and iv) platoon-to-platoon lane change (Wang et al., 2017b). Lee et al. (2014) developed a local coordination scheme that allows three ways to form a platoon: i) front-join, ii) mid-join, and iii) rear-join. Songchitruksa et al. (2016) deployed a local coordination algorithm for CACC evaluation, where only rear-join to a platoon was allowed. Improving from the coordination model of Lee et al., Zhong et al. (2017) implemented the MIXIC (MICROscopic model for Simulation of Intelligent Cruise control) model developed by Van Arem et al. (2006) as a longitudinal control to study the CAV benefits for signalized arterials. The string formation and dispersion mechanism were integrated to the model of Lee et al. in an NCHRP study (Transportation Research Board, 2018), including preferential lane logic and platoon size restriction. A CACC control model was developed by Zhong (2018), where E-IDM (Kesting et al., 2010) was adopted jointly with the MOBIL model (Kesting et al., 2007) that prevents the lane chang-

ing of a free-agent CAV, which may be potentially disruptive to the surrounding traffic. When a potential platooning opportunity is identified via V2V communication, the CACC system estimates the impacts on the immediate vehicles based on MOBIL should the lane change be initiated. The Lane-change Model with Relaxation and Synchronization (LMRS) (Schakel et al., 2012) and the IDM+ (Schakel et al., 2010) were adopted jointly by S. C. Calvert and van Lint (2017) for evaluating the ACC. The LMRS model gives a normalized strategic lane-change score by taking into consideration of route, speed gain, and lane preference. The driver is willing to accept a smaller headway and to decelerate more in LMRS for a higher desire score.

To sum up, microscopic traffic simulation has been widely adopted in assessing the benefits of CACC. Simulation study, however, is not without its caveats, and calibration of the simulation network is one of the them. Besides a proven microscopic behavioral model, the simulation network has to be first calibrated using real-world traffic data to ensure the validity of the simulation results. Not only the global macroscopic traffic flow characteristics (e.g., corridor travel time), but also the local traffic phenomena (e.g., bottlenecks, queues, speed-flow patterns) should be reproduced in the simulation to ensure a good representation of the real-world traffic conditions. Recently studies revealed the shifted attention to evaluating the interaction between CACC and non-equipped vehicles, as well as the operational strategy that can harness the benefits of CACC in mixed traffic conditions. The coordination among CAVs to form vehicular platoons as an operational strategy has shown potential in boosting CACC benefits when the MPR is low. However, its potential negative impact due to induced lane change has not been investigated at the vehicle trajectory level.

3. Evaluation Method

3.1. Simulation of Human Driving Behavior

Human drivers can take into account multiple stimuli (e.g., brake lights, next-nearest neighbors, etc.) with anticipation of the situation for the next few seconds (Treiber and Kesting, 2013). All of these aspects can be formulated into psycho-physiological models, such as the Gipps' model (Gipps, 1981) and the Wiedemann model (PTV Group, 2018; Wiedemann, 1974, 1991).

The Wiedemann model is used by Vissim as the default car-following model. It includes the tactical driving behavior, which carries certain planning in advance with a temporal horizon (multiple time steps) and a spatial horizon that is beyond the neighbor vehicles (Fellendorf and Vortisch, 2010). Such spatial horizon is an augmentation of the initial Wiedemann 74 model in the Vissim car-following behavior, which include ranges of the look-ahead and look-back distances and the numbers of interaction objects/vehicles (PTV Group, 2018). As illustrated in Fig. 2, there are five different driving states in the Wiedemann model: i) free driving, ii) approaching, iii) following, iv) braking, and v) collision. The acceleration is primarily determined by the speed difference (x-axis) and headway/distance (y-axis) to the preceding vehicle for each of the five driving states. The Wiedemann-99 model, suitable for freeway application, has ten calibratable parameters that can constitute a wide range of driver behaviors. Therefore, the Wiedemann model has to be calibrated according to specific traffic stream data (Higgs et al., 2011), as it was initially developed on limited data (Reiter, 1994). The objective of the calibration process is to minimize the difference between the measured driving behavior in the field and the simulated driving behaviors.

When it comes to lateral control, necessary lane change and free lane change are the two types of lane changes in the lateral movement model of Vissim. The former focuses on the hard constraint of the lane change (e.g., lane drop). The latter type is the focus of this study. Such lane change is performed when more space or higher speed is desired for a vehicle. As such, the safety distance plays an important role in lane change behavior, and it is determined based on: i) the speed of the vehicle changing lane, and ii) the approaching speed of the following vehicle (PTV Group, 2018)

3.2. Quantifying Impact to Human Driver

A before-and-after comparison is the most straightforward way to assess the changes that are brought by CAVs. Fig. 3 illustrates the study methodology. First, human driving behavior is calibrated by multiple sources of data that were collected from the roadway segment of interest. Not only the global traffic

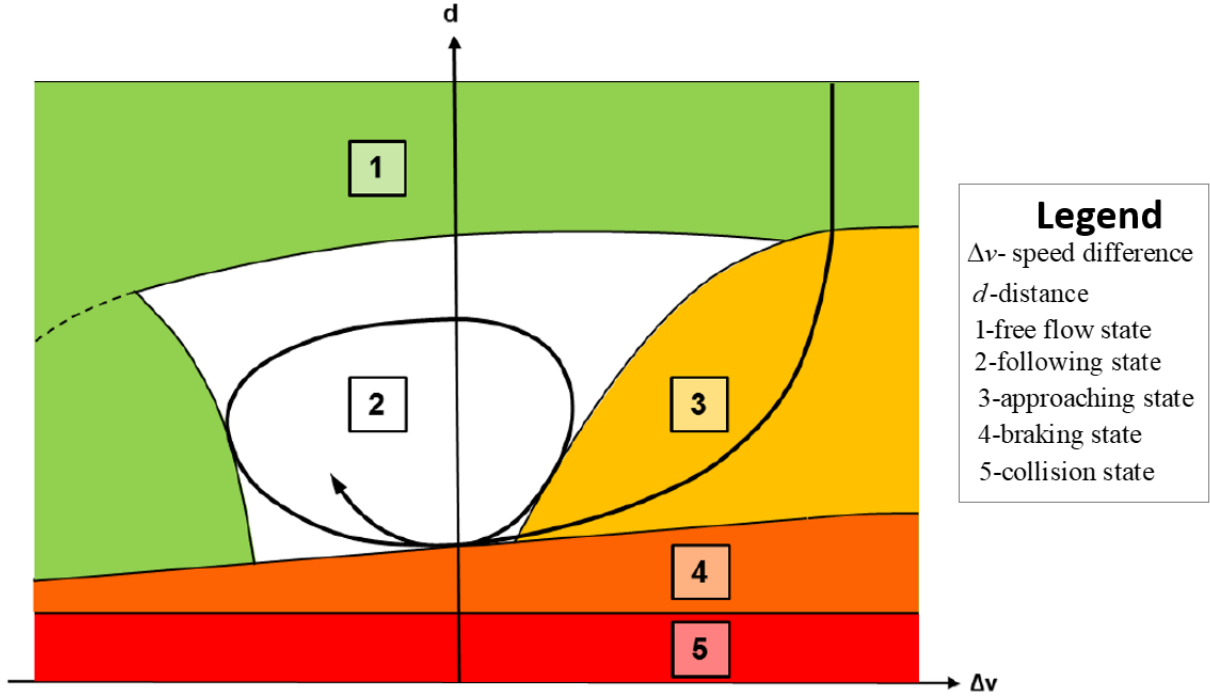


Fig. 2: Wiedemann 1974 model and car-following state (PTV Group, 2018)

characteristics, such as corridor travel time, but also the local traffic patterns (e.g., bottlenecks, queues) were replicated in the simulation. We then treat the car-following model as a plant model. The input is localized traffic conditions, and the output is the reactions of HVs. On a collective level, the traffic flow characteristics and vehicle trajectories are analyzed.



Fig. 3: Potential impact on non-equipped/human-driven vehicles

3.3. Simulation of CAV Driving Behavior

Longitudinal control (or car following) and lateral control are the two main components for simulating the behavior of CACC. The intelligent driver model (IDM) and its variants have been used to design ACC/CACC controller that resembles human-like car-following behaviors (Guérliau et al., 2016; Kesting et al., 2008; Spiliopoulou et al., 2017; Talebpour et al., 2016; Wang et al., 2019b). The Enhanced Intelligent Driver Model (E-IDM) (Kesting et al., 2010) is adopted as the longitudinal control model, which is expressed in Eq. (1).

$$\ddot{x} = \begin{cases} a[1 - (\frac{\dot{x}}{x_{des}})^\delta - (\frac{s^*(\dot{x}, \dot{x}_{lead})}{s_0})] & \text{if } x = \dot{x}_{IDM} \geq \dot{x}_{CAH} \\ (1 - c)\ddot{x}_{IDM} + c[\ddot{x}_{CAH} + b \cdot \tanh(\frac{\dot{x}_{IDM} - \dot{x}_{CAH}}{b})] & \text{otherwise} \end{cases} \quad (1a)$$

$$s^*(\dot{x}, x_{lead}) = s_0 + \dot{x}T + \frac{\dot{x}(\dot{x} - x_{lead})}{2\sqrt{ab}} \quad (1b)$$

$$\ddot{x}_{CAH} = \begin{cases} \frac{\dot{x}^2 \cdot \min(\ddot{x}_{lead}, \ddot{x})}{\ddot{x}_{lead}^2 - 2x \cdot \min(\ddot{x}_{lead}, \ddot{x})} & \dot{x}_{lead}(\dot{x} - \dot{x}_{lead}) \leq -2x \min(\ddot{x}_{lead}, \ddot{x}) \\ \min(\ddot{x}_{lead}, \ddot{x}) - \frac{(\dot{x} - \dot{x}_{lead})^2 \Theta(\dot{x} - \dot{x}_{lead})}{2x} & \text{otherwise} \end{cases} \quad (1c)$$

where, a is the maximum acceleration; b is the desired deceleration; c is the coolness factor; δ is the free acceleration exponent; \dot{x} is the current speed of the subject vehicle; \dot{x}_{des} is the desired speed, \dot{x}_{lead} is the speed of the lead vehicle; s_0 is the minimal distance; \ddot{x} is the acceleration of the subject vehicle; \ddot{x}_{lead} is the acceleration of the lead vehicle; \ddot{x}_{IDM} is the acceleration calculated by the original IDM model (Treiber et al., 2000). The minimal distant can be calculated by Eq. (1b), where T is the desired time gap; and \ddot{x}_{CAH} is the acceleration calculated by the CAH component as shown in Eq. (1c),eq: CAH where Θ is the Heaviside step function. The parameters used for the E-IDM is shown in Table 1. The CAV uses 0.6 s as the desired time gap when following another CAV and 0.9 s otherwise. The desired speed is uniformly distributed between 96 and 105 km/h, and it varies by individual CAV.

Table 1: EIDM Parameters

| Parameter | T | s_0 | a | b | c | θ | \dot{x}_{des} | ϕ_{max} | D_f | D_r |
|-----------|--------------|-------|-------------------|-------------------|------|----------|-----------------|--------------|-------|-------|
| value | 0.6 or 0.9 s | 1m | 2m/s ² | 2m/s ² | 0.99 | 4 | 96~105 km/h | 5 | 20 m | 20 m |

We assume all the CAVs are equipped with automated longitudinal control. Each CACC vehicle is able to detect the surrounding traffic and discern CAVs from HVs. Three cases, as shown in Table 2, are tested.

Table 2: Simulation cases

| Case | Longitudinal Control | Lateral Control |
|---------------------|----------------------|---|
| Base (no CAVs) | calibrated Wiedemann | Vissim |
| Ad hoc coordination | E-IDM | Vissim |
| Local coordination | E-IDM | gap acceptance-based (Lee et al., 2014) |

The lateral control for CACC vehicles in platoon formation was developed by Lee et al. (2014), which has been adopted in multiple studies (FHWA OSDAP, 2015; Transportation Research Board, 2018; Zhong et al., 2017). As demonstrated in Fig. 4, a free-agent CACC vehicle actively communicates with its surrounding vehicles/platoons for platoon formation. Upon the discovery of a platoon opportunity, the free-agent CACC vehicle used its on-board sensors to determine the front and rear gaps based on its lateral projection to the target lane. The lane change is only initiated if both front and rear gaps are above the predetermined thresholds. When the incoming vehicle needs to joint the platoon in the middle, the nearest member within the platoon will decelerate temporarily to create sufficient gaps to facilitate the lane change of the incoming CACC vehicle. The flow chart of the algorithm is provided in Fig. B.1 in Appendix B.

3.4. Case Study Network

In this study, an 8-km (5-mi) segment (Fig. 5) of Interstate Highway I-66 located outside of the beltway (I-495) of Washington D.C. is considered. This freeway segment has recurring congestion during weekdays, specifically in the eastbound direction in the morning and the westbound direction in the afternoon. The roadway has four lanes in each direction. The leftmost lane is an HOV 2+ lane with a peak volume of 1,500 vph per lane (Lu et al., 2014). Currently, there is no physical barrier between the HOV lane and the adjacent general purpose (GP) lane. The calibration was conducted with three independent data sources: INRIX travel time, remote traffic microwave sensor data (RTMS), and video camera data to ensure a realistic representation of the real-world traffic conditions (Leidos, 2016; Li et al., 2019). The first two were the primary sources of fine-tuning the simulation network. The calibration for the Vissim network is further elaborated in Appendix C.

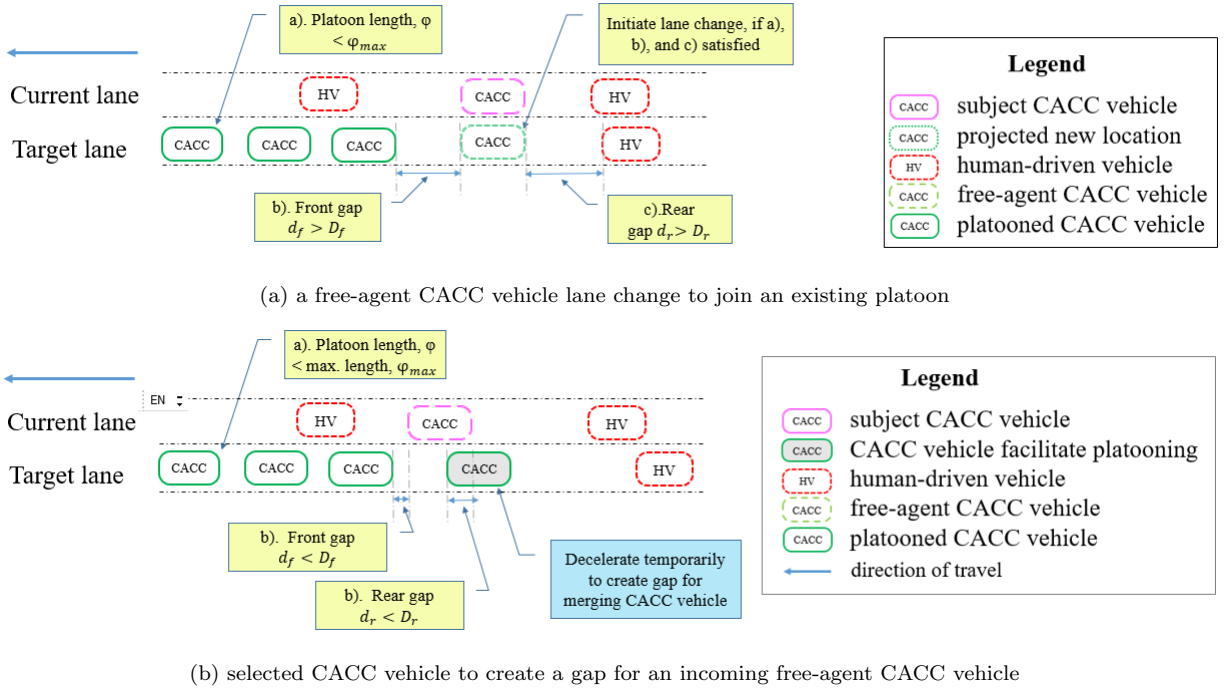


Fig. 4: Local coordination strategy



Fig. 5: I-66 simulation testbed

In anticipation of the increasing traffic demand over time, we assume a 30% increase in the traffic demand from the baseline of the calibrated network. The Wiedemann model in Vissim has stochastic terms, which is implemented via simulation random seed, provided all other parameters unchanged. Therefore, five replications was simulated for each deployment scenario with different random seeds to account for the stochasticity of the traffic conditions. Across the scenarios, the same set of random seeds is used to ensure fair comparison. The duration of the simulation is 3,900 s, the first 300 s of which is used to load the network with traffic. No data is collected during the first 300-s period. The evaluation of the impact is based on the following assumptions:

- A low-level vehicle controller for longitudinal and lateral control is available.
- A calibrated driving behavior model in Vissim with real-world data constitutes a good representation of a subset of the human driver population.
- Vehicle-to-vehicle (V2V) communication is perfect (no interference or packet loss).

- Human drivers do not differentiate CAVs and another HVs in their surrounding, and the behavioral adaptation for CAV behavior (Gouy, 2013) is absent.
- 1.3 times of the original demand is adopted in anticipation of lead-time for CAV deployment.

4. Results & Discussions

The vehicle trajectory data are collected in every 0.5 s. Each simulation replication contains approximately seven million lines of vehicle records, which include not only the vehicle dynamic data but also the interaction states (e.g., driving state and interacting vehicles). A total number of 45 replications are conducted.

4.1. Network Performance

Fig 6(a) shows the ratio of vehicle miles traveled (VMT) and vehicle-hours traveled (VHT). VMT is the output of a transportation system, whereas VHT is considered the input to a transportation system. The ratio of VMT and VHT ratio is referred to as Q (Caltrans Division of Traffic Operations, 2013), which represents the output of a transportation system with the unit value of the input. In short, the higher the value of the Q , the more productive a transportation system is. Either of the ad hoc coordination or local coordination exhibits an increasing trend as the MPR increases. It is notable that the benefits gained by the ad hoc coordination show a diminishing increase after 30% MPR. In comparison, local coordination displays a linear increasing pattern for the performance gain.

When it comes to network throughput, Fig. 6(b) shows that the ad hoc coordination does not increase the network throughput at 10% MPR-the throughput remains as 9,398 vph. Above 10% MPR, the throughput for ad hoc coordination increases with a linear pattern, which matches the underlying operational implication of ad hoc coordination. The throughput reaches the highest 10,167 vph at 40%. With local coordination, additional throughput is observed even at 10% MPR. In addition, the slope of the throughput curve for local coordination is greater at the MPR range between 10% and 30% than other tested MPR values. It also shows that the rate of throughput increment starts to decrease beyond 30% MPR. Moreover, the vertical distance indicates the magnitude that the local coordination outperforms the ad hoc coordination at each level of MPR. The greatest difference is observed at 30% MPR.

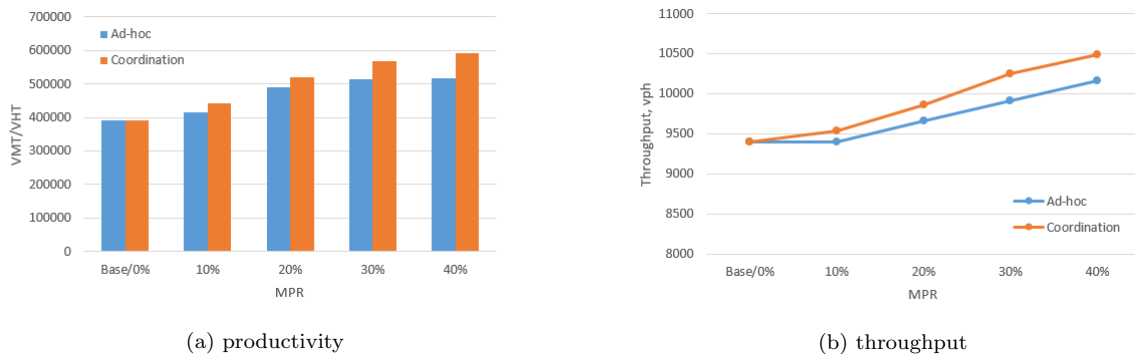


Fig. 6: Network performance

4.2. Hard Braking Observations

Abrupt braking is an indication of a hazardous traffic situation that drivers respond to (Bagdadi and Várhelyi, 2011). Hard braking observations are recorded when the acceleration of a vehicle is less than $-3 m/s^2$. Here, our focus is on the HVs. Based on the interacting vehicle, there are two types of hard braking. The first type occurs when an HV interacts with another HV (HV-HV type interaction); whereas

the second type occurs when an HV interacts with a CAV (HV-CAV type interaction). Fig. 7(a) shows the hard braking observations for HVs when they interact with other HVs. Similar patterns of the cumulative distribution functions (CDFs) for hard braking are observed across the testing scenarios. Fig. 7(b) shows the number of observations for each scenarios. The primary factor for the decreasing trend is the reduction of HVs in the traffic stream. The linear trend also infers that the likelihood of hard braking remains at the same level.

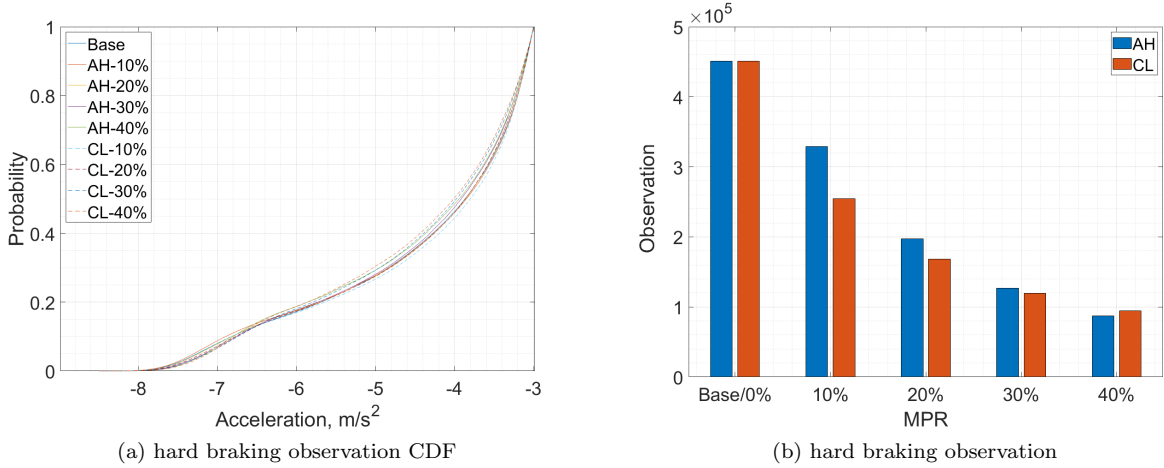


Fig. 7: Hard braking observation when interacting with HVs

Fig. 8(a) shows the CDFs of the hard braking observations recorded for HVs when they interact with CAVs. The CDFs show two distinctive patterns between two coordination strategies. In the ad hoc coordination case, the CDFs are with similar distributions. On the other hand, the CDFs of local coordination are more sensitive to MPR. The probability of hard braking between $-6.5 m/s^2$ and $-3.5 m/s^2$ increases drastically even at 10% MPR. The occurrence of hard braking events keeps at the same level in ad hoc coordination; whereas the occurrence of coordination strategy shows an increasing trend until reaching 30% MPR. The number of observations is shown in Fig. 8(b). Both strategies exhibit an increasing trend, then a declining trend after 30% MPR. With the same amount of CAVs, the hard braking is more sensitive to MPR in local coordination than that in the ad hoc coordination.

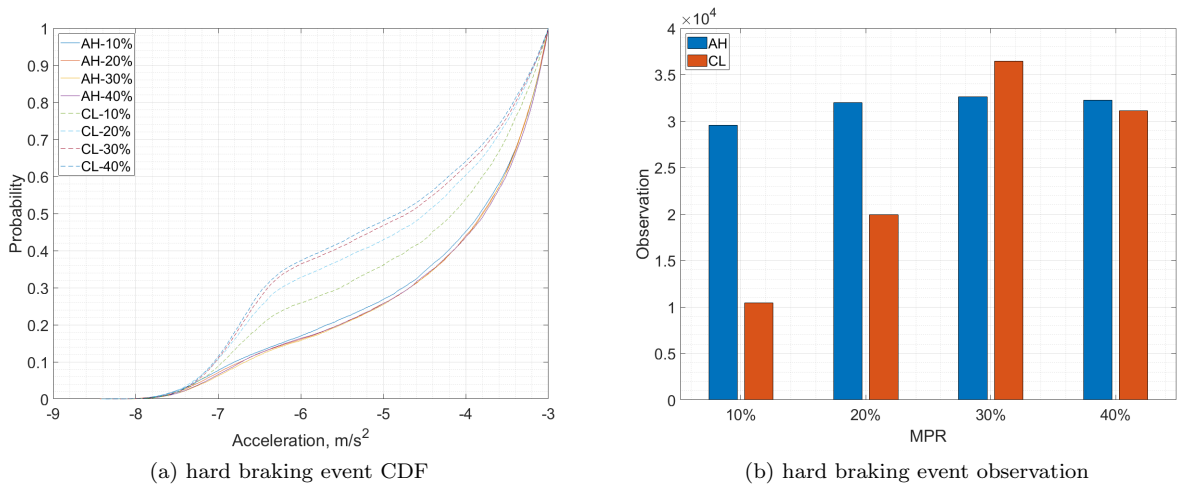


Fig. 8: Hard braking event when interacting with CAVs

Two-sample Kolmogorov-Smirnov (K-S) test is adopted to further analyze the CDFs. The K-S test is a powerful tool for testing the hypothesis of whether two random samples have been drawn from the same population (Goodman, 1954). It is a non-parametric test where no assumption is made regarding the distribution of the variables (Young, 1977). The null hypothesis (H_0) of the K-S test is that the comparing two sample sets are from the same continuous distribution. Table 3 shows the result of the two-sample K-S test for the hard braking CDFs for HVs. The value of “1” represents that the null hypothesis is rejected at a 5% significance level. As shown, any pair of the scenarios rejects the null hypothesis and accept the alternative hypothesis that the two samples are not from the same distribution. The observations only fail to reject the H_0 in the ad hoc coordination case at 20% and 30% MPR .

Table 3: Two-sample K-S test for Hard Braking

| | A-10% | A-20% | A-30% | A-40% | C-10% | C-20% | C-30% | C-40% |
|-------|-------|-------|-------|-------|-------|-------|-------|-------|
| A-10% | - | 1 | 1 | 1 | 1 | 1 | 1 | 1 |
| A-20% | 1 | - | 0 | 1 | 1 | 1 | 1 | 1 |
| A-30% | 1 | 0 | - | 1 | 1 | 1 | 1 | 1 |
| A-40% | 1 | 1 | 1 | - | 1 | 1 | 1 | 1 |
| C-10% | 1 | 1 | 1 | 1 | - | 1 | 1 | 1 |
| C-20% | 1 | 1 | 1 | 1 | 1 | - | 1 | 1 |
| C-30% | 1 | 1 | 1 | 1 | 1 | 1 | - | 1 |
| C-40% | 1 | 1 | 1 | 1 | 1 | 1 | 1 | - |

4.3. Safety Surrogate Assessment Measure

The Surrogate Safety Assessment Model (SSAM) is a tool for identifying traffic conflicts from vehicle trajectories (Gettman et al., 2008). The time to collision (TTC) less than 3 s to a preceding vehicle for each HV is extracted from the trajectory data. Fig. 9 (a) shows the TTC for HV-HV type interaction and Fig. 9 (b) shows the HV-CAV interaction. Like hard braking, we performed the two-sample K-S test for each pair of CDFs and found that all the comparisons reject the null hypothesis. Then we examined the CDF portion where TTC is under 1.5 s. For the HV-HV type interaction, the cumulative probability increase along with the MPR. For the HV-CAV type interaction, the probability of TTC less than 1-s is higher with local coordination except at 10% MPR, and the cumulative probability is higher as the MPR grows. Under ad hoc strategy, the cumulative probability slightly increases when TTC is less than 0.8 s, and then they fall below the Base CDF curve between 1 s and 1.6 s.

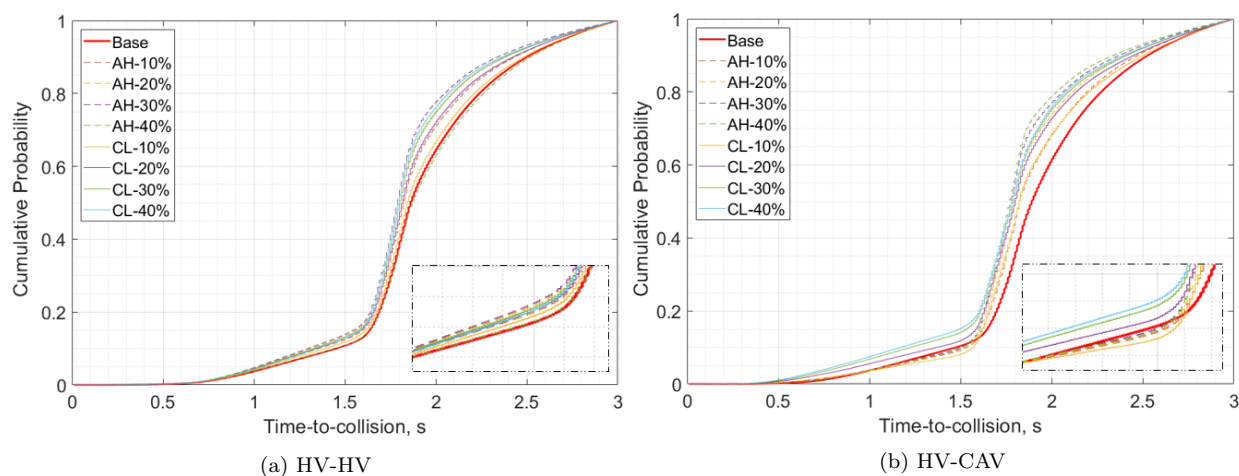


Fig. 9: Time-to-collision (TTC) CDF

4.4. Lane Change Activities

Fig. 10 shows the accumulative lane change recorded at every 0.5 s for all HVs. As mentioned previously, the Vissim has a necessary lane change and free lane change in its default model. The lane change activity decreases as the MPR of CACC increases in either of the coordination strategies. Local coordination is marginally higher than the ad hoc one when the MPR is low. At 40% MPR, they reach the same level of lane change activity. However, recall that the number of HV within the network decreases as the MPR of CACC increases. The average lane change frequency for each HV is plotted in Fig.10 as well. The local coordination strategy shows a higher average lane change frequency at 10% and 20% MPR. The average lane change frequency peaks at 30%, then reduced to 5.38 from 5.42 per vehicle. On the contrary, the increasing trend for ad hoc coordination keeps increasing and reach 5.46 and 5.48 per vehicle at 30% and 40%, respectively. 30% is the stationary point when it comes to average lane change frequency. The surrounding CAV could induce HVs for more lane change for greater space or higher speed. Some examples for the reaction of HVs include: i) the high traffic density resulted from the closely-coupled CACC platoon, ii) the short following distance under which a CAV can be safely operated, iii) the narrower gap for CAV lane change could encroach the desired headway for HV, hence prompts HV’s lane change

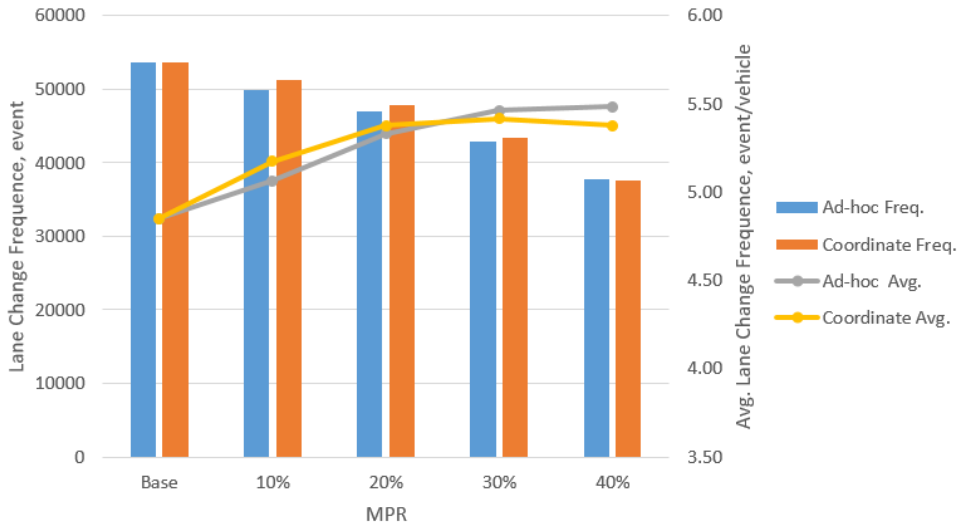


Fig. 10: Lane change activity of HVs

4.5. Interaction State

The Wiedenmann model assumes five basic interaction states for a human driver. The Braking and Collision states are often coded as “Brake BX” and “Brake AX,” respectively. The former represents braking performed before reaching the safety distance, whereas the latter represents braking performed after reaching the safety distance. The definition of each interaction state is listed in Table 4. The transition to one state to another is triggered by a threshold, which can be expressed as a function of the speed difference and distance (PTV Group, 2018).

Table 4: Wiedenmann’s car-following interaction state

| Parameter | Definition |
|-----------|---|
| Free | a vehicle is not affected by any relevant preceding vehicle. It tries to drive at its desired speed |
| Close-up | a vehicle is reaching an obstacle (e.g., signal head, vehicle, conflict area) |
| Follow | a vehicle tries to follow a leading vehicle |
| Brake BX | braking at the desired safety distance before reaching the safety distance |
| Brake AX | braking after reaching the safety distance |

The high-resolution trajectory data contains the interaction state information, which provides insights for the influence of CAVs on HVs. By analyzing the interaction data, we can quantify the possible influence of CAV. The composition of the interaction state is shown in Fig. 11. The non-major interaction states are grouped into a new category-“Other”. The percentage of “Free” state for HVs is higher in the local coordination strategy at each level of MPR compared to its counterparts. In the “Base” case, on average 37% of the time the HVs are driving under “Free” condition. The introduction of CAVs with ad hoc strategy only marginally increases the percentage of “Free” condition for HVs. When implementing the Coordination strategy, the percentage of “Free” condition gains a greater increase, and it reaches 48% at 40% MPR.

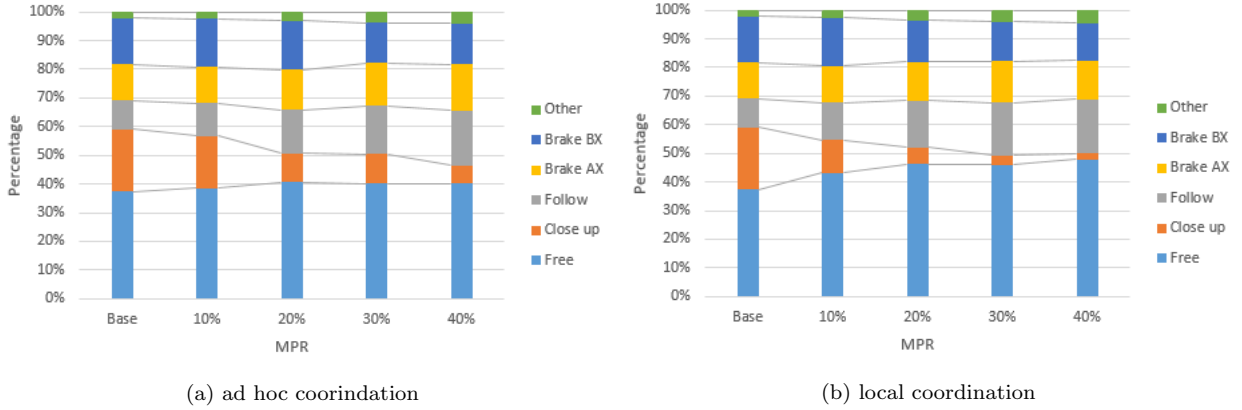


Fig. 11: Composition of interaction state for HVs

The “Close-up” and “Follow” states are isolated and shown in Fig. 12(a). The percentage of the “Close-up” state exhibits a decreasing trend as the MPR increases. With the local coordination strategy, the time HV spent in the “Close-up” state decline more rapidly as the MPR increases. It is also observed that HVs spend more time in the “Follow” state when CAVs use local coordination strategy. The increased percentage of the “Follow” state indicates a shorter time headway on average. Recall in Fig. 6(b) that the throughput is increased with CAVs. Therefore the density of the traffic is increased, resulting in a shorter headway on average and more time in Follow state. Fig. 12(b) details the compositions of the two braking states. The “Brake AX” state has more significant safety implications, as it reflects the braking that is performed after a reaching safety distance. The observations for the “Brake AX” reach the highest 17% (at 40% MPR) and 15% (at 30% MPR) for ad hoc coordination and local coordination strategies, respectively. The “Brake AX” increases monotonically in Ad hoc case; whereas it decreases back to 14% after the peak.

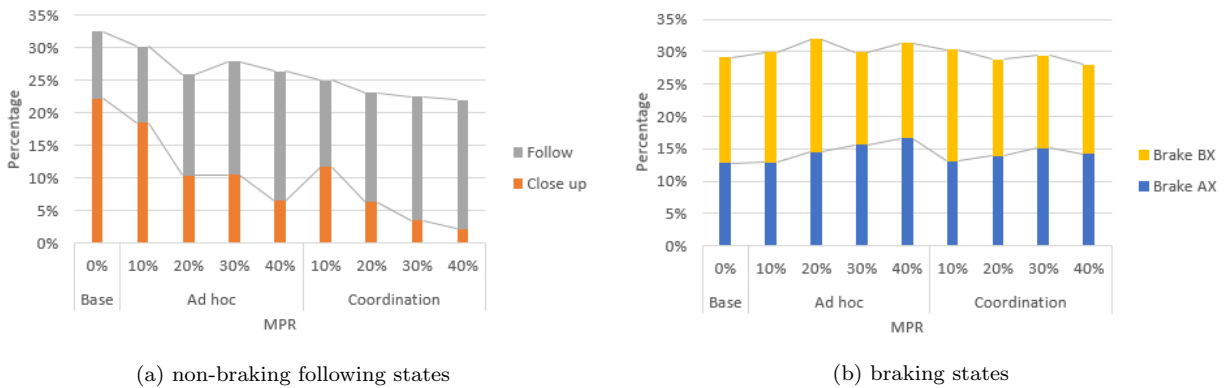


Fig. 12: Interaction state for HV

Fig. 13(a) shows the speed difference-headway plot, which imitates the theoretical plot in Fig. 2. Each vehicle slightly varies in the separation of the five following states, depending on the random seed. Due to a large number of observations, overlapping among sample points is hard to avoid, especially for the same following state sharing the same color. Fig. 13(b) displays the speed difference-acceleration plot. It shows that the disappearance of the observation of the “Close-up” state as MPR increases for both strategies. The reduction is greater in the local coordination case, which is consistent with the trend shown in Fig. 12(a).

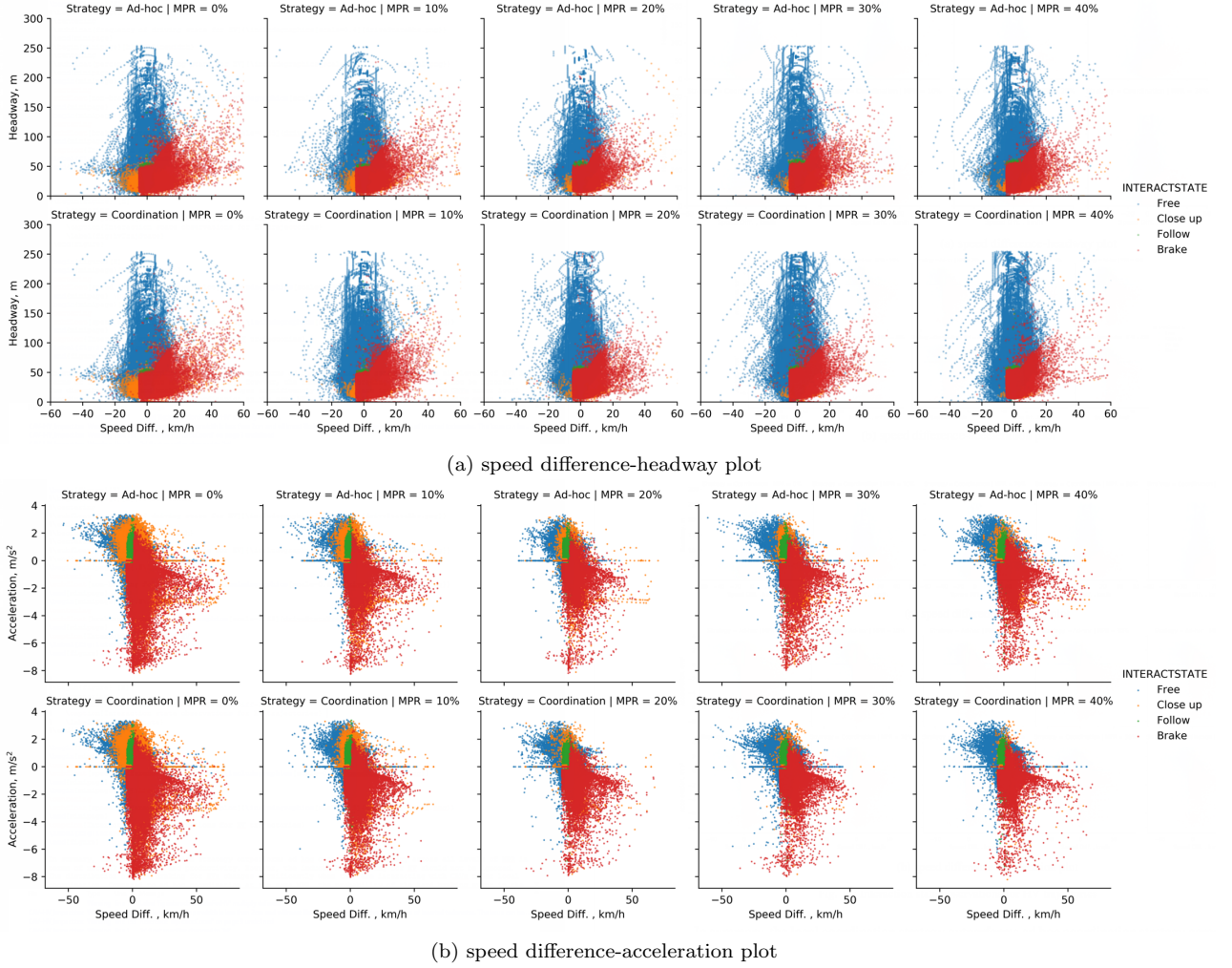


Fig. 13: Interaction state observations for HV trajectories

In summary, the local coordination strategy outperforms ad hoc coordination strategy across all levels of MPR in terms of network throughput and productivity. However, the induced hard braking for HV should not be overlooked. The distribution of hard braking for HVs changes significantly when they are interacting with CAVs under local coordination. Compared to ad hoc coordination at the same MPR, the probability of the hard braking event in the range between $-7.3 m/s^2$ and $-6.5 m/s^2$ is higher. The local coordination causes a higher average lane change frequency for HV at low MPRs (i.e., 10% and 20%). It starts to decrease after reaching 30% MPR, whereas in the ad hoc coordination the average lane change frequency maintains the increasing trend. The interaction state of the calibrated car-following model for HVs also reveals an interesting pattern. The local coordination yields a higher percentage of “Free” interaction state than ad hoc coordination. The “Close-up” state experience a greater reduction in the local coordination strategy,

probably due to the shorter following headway, which is also supported by the increase of the “Follow” state. The percentage of the “Follow” state is positively correlated to the MPR of CAVs. With denser traffic flow, it is logical that the more time HVs as a group spend an additional amount of time in the “Follow” state.

5. Conclusions

In this paper, we investigate the two types of clustering strategies for forming CAV platoons. Platoon clustering strategy is of significant importance when it comes to deploying CAV in mixed traffic conditions in the near term. In agreement with most previous studies, CAVs are able to bring benefits to the transportation network with ad hoc coordination, and adapting local coordination can further increase the benefits. In addition, we quantify the impacts of CAV clustering strategies on HVs. The distribution of the hard braking for HVs, when interacting with CAVs, changes significantly with local coordination strategy for platoon formation. In comparison, the distributions for HVs, when interacting with other HVs, does not show significant changes. The average lane change for HVs increases with the presence of CAVs until 30% MPR is reached. The analysis of the interaction state of the vehicle trajectory data reveals the different impacts of coordination strategy as well. It is shown that the percentage of “Free” driving can be increased by the introduction of CAV with local coordination strategy.

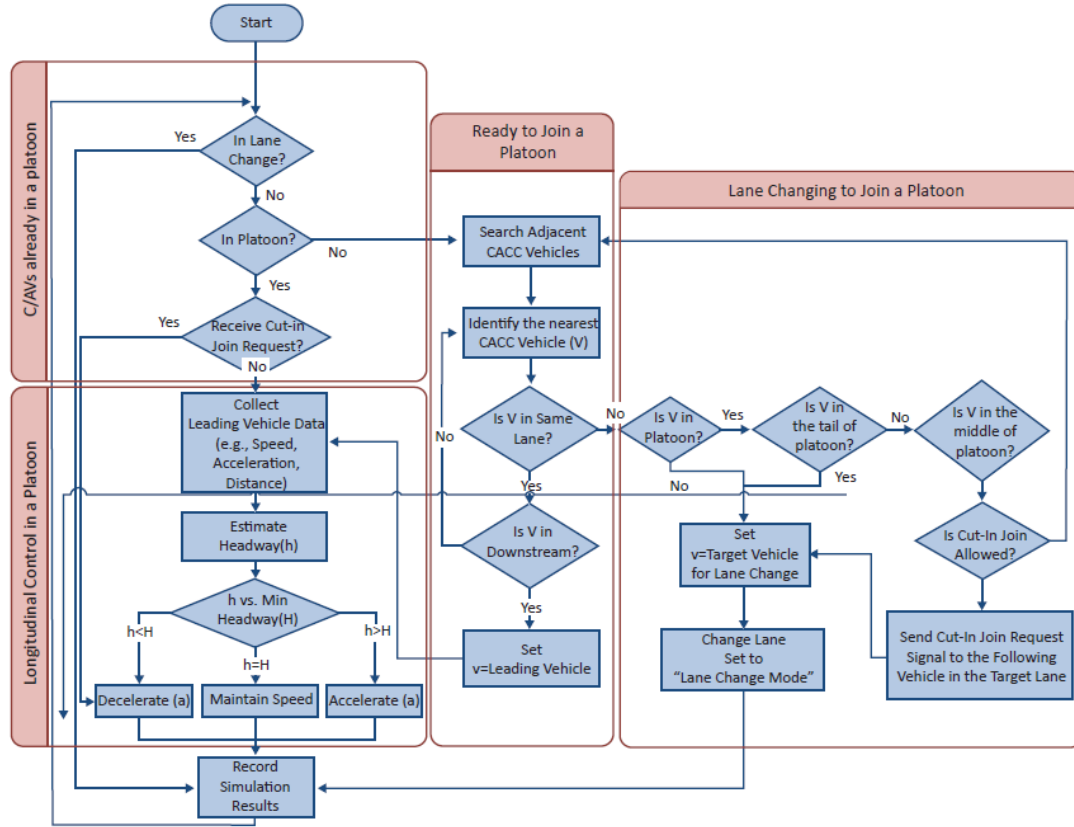
Nevertheless, there are some limitations with regard to this study. First, the E-IDM, while being widely adopted, lacks the multi-anticipative car-following characteristic that has been promoted as one of the crucial feature enabled by V2V communication. However, the longitudinal control of CAVs is not the focus of this study, and the local coordination is predominately associated with the lateral control of CAVs. Second, the simulation network was calibrated using the field data collected at the northern Virginia, which only represents a subset of the overall driver population. Regional variability could exist among different subsets of drivers. Future research may focus on the following areas. The lateral control is an under-explored area compared to longitudinal control of CAVs. Further investigation of platoon formation in mixed traffic is desired. Currently, there are only a few platoon coordination algorithms, most of which are rule-based. Furthermore, the aggressiveness of the lane change for CAVs during platoon formation is also an important aspect. As shown in this paper, the characteristics of the HV traffic could be influenced, and some of CAV maneuvers during clustering could even pose safety concerns for HVs. Lastly, the comparison among clustering strategies should be further expanded with additional scenarios. Cross validation of different models for CAVs and/or HVs, as well as the comparison of corresponding results should be conducted in the future study, since the nature of the CAV behavior is still at a developmental stage.

Appendix A. List of Abbreviations

Table A1: List of Abbreviations

| Abbreviation | Definition |
|---------------------|--|
| ACC | adaptive cruise control |
| AH | ad hoc |
| AV | automated vehicles |
| CAV | connected and automated vehicles |
| CACC | cooperative adaptive cruise control |
| CAH | constant acceleration heuristic |
| CDF | cumulative distribution function |
| CL | local coordination |
| E-IDM | enhanced intelligent driver model |
| GP | general purpose |
| HOV | high-occupancy vehicle |
| HV | human-driven vehicle |
| LMRS | Lane-change Model with Relaxation and Synchronization |
| MPR | market penetration rate |
| MIXIC | MICROscopic model for Simulation of Intelligent Cruise control |
| MOBIL | minimizing overall braking induced by lane change |
| NHCRP | National Highway Cooperative Research Program |
| OSDAP | Open Source Application Development Portal |
| SARTRE | Safe Road Trains for the Environment project |
| SSAM | safety surrogate assessment model |
| TTC | time to collision |
| VAD | vehicle awareness device |
| VMT | vehicle mile traveled |
| VHT | vehicle hour traveled |

Appendix B. CAV Local Coordination Flowchart



Source: Lee et al. (2014).

Fig. B.1: Flowchart for CACC local coordination (Lee et al., 2014; Transportation Research Board, 2018)

Appendix C. Simulation Calibration

The data collected from the field for calibration were RTMS (remote traffic microwave sensor), INRIX probe vehicle travel time data, and video camera footage. Each data source is independent and the associated traffic flow metrics are shown in Table A2.

Table A2: Independent Data Source for Calibration

| Data Source | Volume | Speed | Occupancy | Travel Time | Measurement Type |
|----------------------|--------|-------|-----------|-------------|------------------|
| RTMS data | ✓ | ✓ | ✓ | | point |
| INRIX data | | | | ✓ | segment |
| Video camera footage | ✓ | | | | point |

Appendix C.1. Origin-destination Demand

The QueensOD (Rakha, 2002), a software application for estimating time-dependent static O-D, was used to estimate the volumes of the OD pairs that do not have sensor coverage. The results were then compared with field observations at a 15-min interval. Fig. C.2 displays two of the total 16 intervals for the I-66 Vissim network.

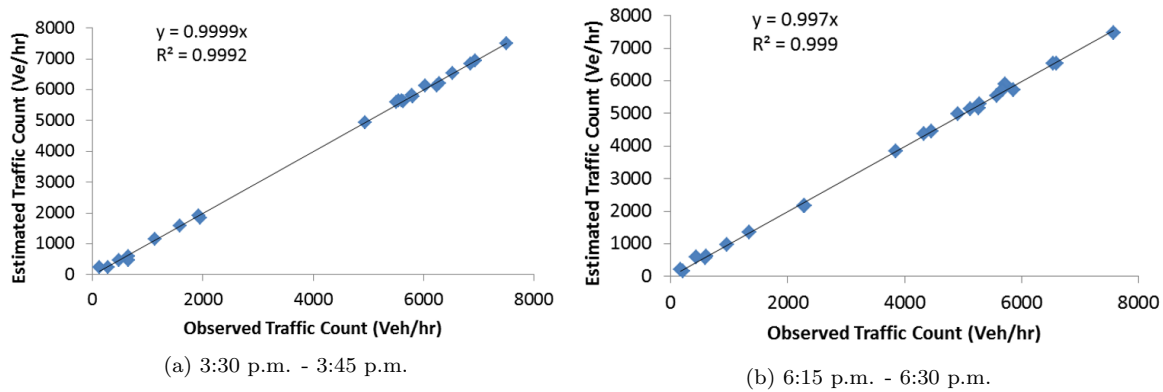


Fig. C.2: Calibration for OD demand

Appendix C.2. Traffic flow characteristics

With the estimated values for all OD pairs, the Latin Hypercube Sampling was adopted to generate hundreds of scenarios for Vissim evaluation in order to narrow down parameters set candidates. Then the selected candidates were fine-tuned by adjusting the driving behaviors in multiple locations to reflect the traffic flow characteristics across multiple segments in the network. Figure C.3 compares the traffic flow characteristics of the two RTMS locations between the field and the simulation at the two RTMS locations.

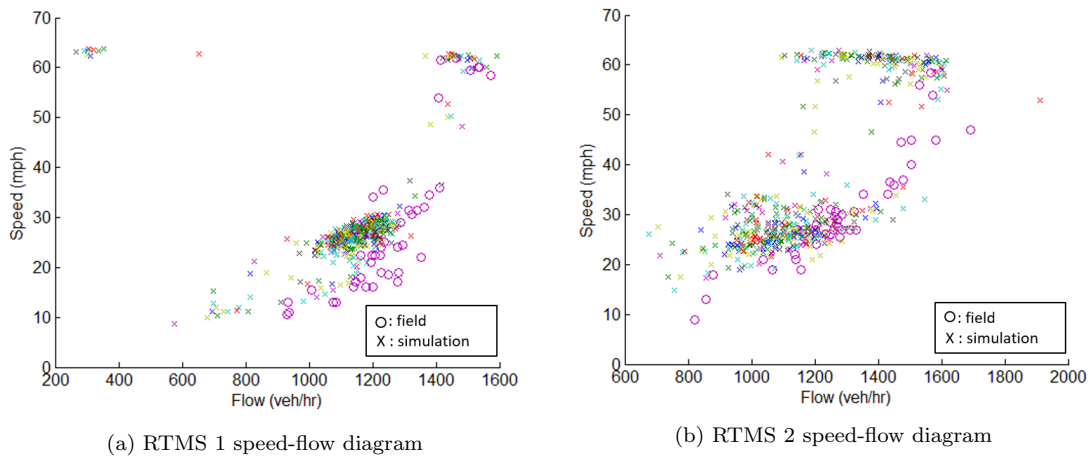


Fig. C.3: Calibration for traffic flow characteristics

The TMC segments shown in Table A3 were also calibrated. The field travel time from 3:30 p.m. to 6:30 p.m. on Nov. 12, 2014, was used. Note that the daily variance of the travel time was not taken into account in this calibration.

Table A3: INRIX TMC Segments

| TMC Code | From (exit, latitude, longitude) | | | To (exit, latitude, longitude) | | | Mileage |
|-----------|----------------------------------|----------|----------|--------------------------------|----------|----------|---------|
| 110+04176 | I-495/EXIT 64 | 38.88308 | -77.2295 | VA-243/NUTLEY ST/EXIT 62 | 38.87883 | -77.2628 | 1.8 |
| 110P04176 | I-495/EXIT 64 | 38.87883 | -77.2628 | VA-243/NUTLEY ST/EXIT 62 | 38.87824 | -77.2703 | 0.4 |
| 110+04177 | VADEN DR/ EXIT 62 | 38.87824 | -77.2703 | VA-123/EXIT 60 | 38.87741 | -77.2748 | 0.3 |
| 110+04178 | VA-243/NUTLEY ST/EXIT 62 | 38.87741 | -77.2748 | VA-123/EXIT 60 | 38.8704 | -77.3006 | 1.4 |

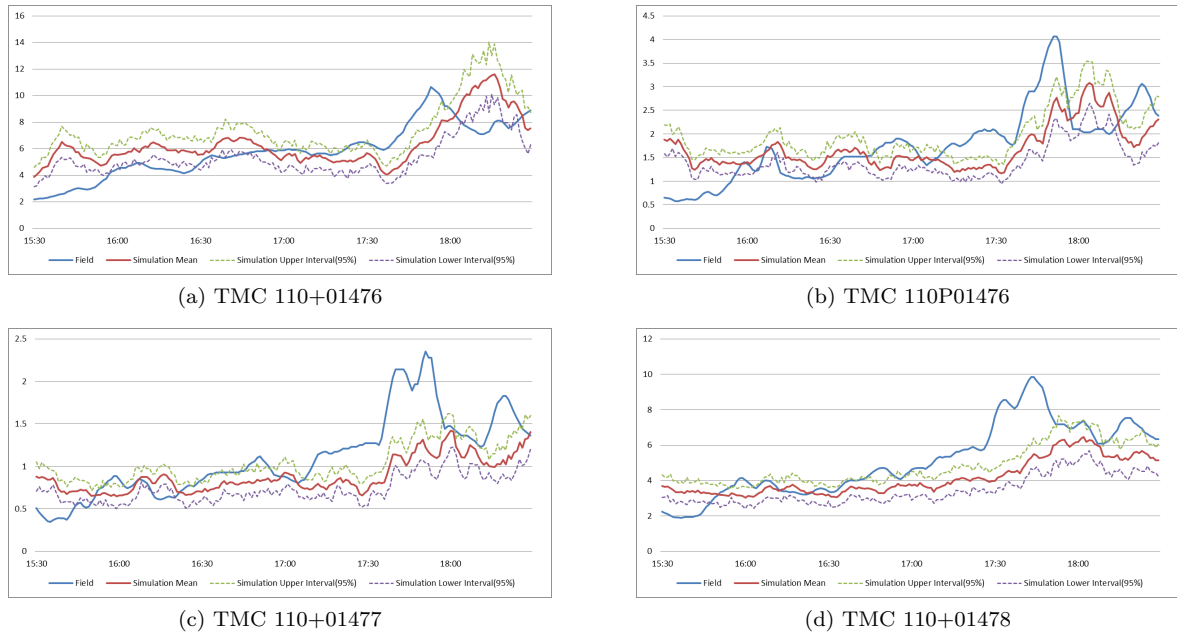


Fig. C.4: Calibration for TMC travel time

For the deceleration profile, we used the Vissim default profile for passenger cars, which has the maximum deceleration of -8.5 m/s^2 . The default profile for maximum deceleration for passenger cars corresponds to those established in the traffic flow model Wiedemann 74. The parameters were measured in Germany, then later, a slight change for shorter time step with a constraint on jerk was adopted (PTV Group, 2018). The range, when applicable, of the most influential parameters for the Wiedemann 99 model is shown in Table A4, which are calibration based on the field data collected in northern Virginia in the United States.

Table A4: Independent Data Source for Calibration

| Wiedemann 99 parameter | Value range |
|--------------------------------|-------------|
| CC0 (standstill distance) | 1.5 m |
| CC1 (following distance) | 0.5 -1.5 s |
| CC2 (longitudinal oscillation) | 3 - 4 m |

References

- Aarts, L., Feddes, G., 2016. European truck platooning challenge. In: International Symposium on Heavy Vehicle Transport Technology (HVTT14), Rotorua, New Zealand.
- Amirgholy, M., Shahabi, M., Gao, H. O., 2020. Traffic automation and lane management for communicant, autonomous, and human-driven vehicles. *Transportation Research Part C: Emerging Technologies* 111, 477 – 495.
URL <http://www.sciencedirect.com/science/article/pii/S0968090X18315791>
- Arnaout, G. M., Arnaout, J.-P., 2014. Exploring the effects of cooperative adaptive cruise control on highway traffic flow using microscopic traffic simulation. *Transportation Planning and Technology* 37 (2), 186–199.
URL <https://doi.org/10.1080/03081060.2013.870791>
- Bagdadi, O., Várhelyi, A., 2011. Jerky driving—an indicator of accident proneness? *Accident Analysis & Prevention* 43 (4), 1359–1363.
- Berghöfer, F. L., Purucker, C., Naujoks, F., Wiedemann, K., Marberger, C., 2018. Prediction of take-over time demand in conditionally automated driving-results of a real world driving study. In: *Proceedings of the Human Factors and Ergonomics Society Europe Chapter 2018 Annual Conference*. pp. 69–81.
- Caltrans Division of Traffic Operations, 2013. A guide to using the caltrans performance measurement system (PeMS) in transportation concept reports. Tech. rep.

- Casey, S. M., Lund, A. K., 1992. Changes in speed and speed adaptation following increase in national maximum speed limit. *Journal of Safety Research* 23 (3), 135 – 146.
URL <http://www.sciencedirect.com/science/article/pii/0022437592900163>
- Chan, E., 2016. SARTRE Automated Platooning Vehicles. John Wiley and Sons, Ltd, Ch. 10, pp. 137–150.
URL <https://onlinelibrary.wiley.com/doi/abs/10.1002/9781119307785.ch10>
- Chang, J., Fok, E., et al., 2018. Connected vehicle pilot positioning and timing report: Summary of positioning and timing approaches in CV pilot sites. Tech. rep., United States. Dept. of Transportation. ITS Joint Program Office.
- Eilers, S., Mårtensson, J., Pettersson, H., Pillado, M., Gallegos, D., Tobar, M., Johansson, K. H., Ma, X., Friedrichs, T., Borojeni, S. S., et al., 2015. Companion—towards co-operative platoon management of heavy-duty vehicles. In: 2015 IEEE 18th International Conference on Intelligent Transportation Systems. IEEE, pp. 1267–1273.
- Fairclough, S. H., May, A. J., Carter, C., 1997. The effect of time headway feedback on following behaviour. *Accident Analysis & Prevention* 29 (3), 387 – 397.
URL <http://www.sciencedirect.com/science/article/pii/S0001457597000055>
- Fellendorf, M., Vortisch, P., 2010. Microscopic traffic flow simulator Vissim. In: *Fundamentals of traffic simulation*. Springer, pp. 63–93.
- FHWA OSDAP, 2015. Vissim external driver model (VEDM) add-on for connected automated vehicle (CAV) applications now available for download.
URL <https://www.itsforge.net/index.php/vedm-cac-announced>
- Gettman, D., Pu, L., Sayed, T., Shelby, S., 2008. Surrogate safety assessment model and validation: Final report. Publication No. FHWA-HRT-08 51.
- Ghiasi, A., Hussain, O., Qian, Z. S., Li, X., 2017. A mixed traffic capacity analysis and lane management model for connected automated vehicles: A markov chain method. *Transportation Research Part B: Methodological* 106, 266 – 292.
URL <http://www.sciencedirect.com/science/article/pii/S0191261517302278>
- Ghiasi, A., Li, X., Ma, J., 2019. A mixed traffic speed harmonization model with connected autonomous vehicles. *Transportation Research Part C: Emerging Technologies* 104, 210 – 233.
URL <http://www.sciencedirect.com/science/article/pii/S0968090X18304169>
- Gipps, P., 1981. A behavioural car-following model for computer simulation. *Transportation Research Part B: Methodological* 15 (2), 105 – 111.
URL <http://www.sciencedirect.com/science/article/pii/0191261581900370>
- Goodman, L. A., 1954. Kolmogorov-smirnov tests for psychological research. *Psychological bulletin* 51 (2), 160.
- Gouy, M., 2013. Behavioural adaptation of drivers of unequipped vehicles to short time headways observed in a vehicle platoon. Ph.D. thesis, The Open University.
- Gouy, M., Wiedemann, K., Stevens, A., Brunett, G., Reed, N., 2014. Driving next to automated vehicle platoons: How do short time headways influence non-platoon drivers’ longitudinal control? *Transportation Research Part F: Traffic Psychology and Behaviour* 27, 264 – 273.
URL <http://www.sciencedirect.com/science/article/pii/S1369847814000345>
- Guériau, M., Billot, R., Faouzi, N.-E. E., Monteil, J., Armetta, F., Hassas, S., 2016. How to assess the benefits of connected vehicles? a simulation framework for the design of cooperative traffic management strategies. *Transportation Research Part C: Emerging Technologies* 67, 266 – 279.
URL <http://www.sciencedirect.com/science/article/pii/S0968090X16000462>
- Higgs, B., Abbas, M. M., Medina, A., 2011. Analysis of the Wiedemann car following model over different speeds using naturalistic data. In: *Procedia of RSS Conference*. pp. 1–22.
- Hussain, O., Ghiasi, A., Li, X., 2016. Freeway lane management approach in mixed traffic environment with connected autonomous vehicles. arXiv preprint arXiv:1609.02946.
- Kesting, A., Treiber, M., Helbing, D., 2007. General lane-changing model MOBIL for car-following models. *Transportation Research Record* 1999, 86–94.
URL <http://trrjournalonline.trb.org/doi/10.3141/1999-10>
- Kesting, A., Treiber, M., Helbing, D., 2010. Enhanced intelligent driver model to access the impact of driving strategies on traffic capacity. *Philosophical Transactions of the Royal Society A: Mathematical, Physical and Engineering Sciences* 368 (1928), 4585–4605.
- Kesting, A., Treiber, M., Schönhof, M., Helbing, D., 2008. Adaptive cruise control design for active congestion avoidance. *Transportation Research Part C: Emerging Technologies* 16 (6), 668 – 683.
URL <http://www.sciencedirect.com/science/article/pii/S0968090X08000028>
- Lank, C., Haberstroh, M., Wille, M., 2011. Interaction of human, machine, and environment in automated driving systems. *Transportation Research Record* 2243 (1), 138–145.
URL <https://doi.org/10.3141/2243-16>
- Lee, J., Bared, J., Park, B., 2014. Mobility impacts of cooperative adaptive cruise control (CACC) under mixed traffic conditions. In: 93rd Annual Meeting of the Transportation Research Board, Washington, DC.
- Lee, S., Jeong, E., Oh, M., Oh, C., 2019. Driving aggressiveness management policy to enhance the performance of mixed traffic conditions in automated driving environments. *Transportation Research Part A: Policy and Practice* 121, 136 – 146.
URL <http://www.sciencedirect.com/science/article/pii/S0965856418304063>
- Leidos, 2016. Simulation of evolutionary introduction of cooperative adaptive cruise control equipped vehicles into traffic. Tech. rep., Saxton Transportation Operations Laboratory.
- Li, T., Ma, J., Hale, D. K., 2019. High-occupancy vehicle lanes on the right: an alternative design for congestion reduction at freeway merge, diverge, and weaving areas. *Transportation Letters* 0 (0), 1–13.

- URL <https://doi.org/10.1080/19427867.2019.1584347>
- Liu, H., Kan, X. D., Shladover, S. E., Lu, X.-Y., Ferlis, R. E., 2018. Modeling impacts of cooperative adaptive cruise control on mixed traffic flow in multi-lane freeway facilities. *Transportation Research Part C: Emerging Technologies* 95, 261 – 279. URL <http://www.sciencedirect.com/science/article/pii/S0968090X18310313>
- Lu, X.-Y., Lee, J., Chen, D., Bared, J., Dailey, D., Shladover, S. E., 2014. Freeway micro-simulation calibration: Case study using Aimsun and Vissim with detailed field data. In: 93rd Annual Meeting of the Transportation Research Board, Washington, DC.
- Ma, J., Hu, J., Leslie, E., Zhou, F., Huang, P., Bared, J., 2019. An eco-drive experiment on rolling terrains for fuel consumption optimization with connected automated vehicles. *Transportation Research Part C: Emerging Technologies* 100, 125 – 141. URL <http://www.sciencedirect.com/science/article/pii/S0968090X18300561>
- Milanés, V., Shladover, S. E., 2014. Modeling cooperative and autonomous adaptive cruise control dynamic responses using experimental data. *Transportation Research Part C: Emerging Technologies* 48, 285 – 300. URL <http://www.sciencedirect.com/science/article/pii/S0968090X14002447>
- Naujoks, F., Purucker, C., Wiedemann, K., Neukum, A., Wolter, S., Steiger, R., 2017. Driving performance at lateral system limits during partially automated driving. *Accident Analysis & Prevention* 108, 147–162.
- Nowakowski, C., O’Connell, J., Shladover, S. E., Cody, D., 2010. Cooperative adaptive cruise control: Driver acceptance of following gap settings less than one second. In: *Proceedings of the Human Factors and Ergonomics Society Annual Meeting*. Vol. 54. SAGE Publications Sage CA: Los Angeles, CA, pp. 2033–2037.
- Nowakowski, C., Shladover, S. E., Cody, D., Bu, F., O’Connell, J., Spring, J., Dickey, S., Nelson, D., 2011. Cooperative adaptive cruise control: Testing drivers’ choices of following distances. Tech. rep.
- Papadoulis, A., Quddus, M., Imprialou, M., 2019. Evaluating the safety impact of connected and autonomous vehicles on motorways. *Accident Analysis & Prevention* 124, 12 – 22. URL <http://www.sciencedirect.com/science/article/pii/S0001457518306018>
- PTV Group, 2018. PTV Vissim 11 user manual. Germany: PTV GROUP.
- Qom, S. F., Xiao, Y., Hadi, M., 2016. Evaluation of cooperative adaptive cruise control (CACC) vehicles on managed lanes utilizing macroscopic and mesoscopic simulation. In: *Transportation Research Board 95th Annual Meeting*. No. 16-6384.
- Rakha, H., 2002. *Queensod rel. 2.10-user’s guide: Estimating origin-destination traffic demands from link flow counts*. ed: Michel Van Aerde & Associates Ltd., Blacksburg, VA.
- Reiter, U., 1994. Empirical studies as basis for traffic flow models. In: *Proceedings of the 2nd International Symposium on Highway Capacity*, Vol. 2.
- S. C. Calvert, W. J. S., van Lint, J. W. C., 2017. Will automated vehicles negatively impact traffic flow. *Journal of Advanced Transportation* 2017.
- Saha, P., Roy, R., Sarkar, A. K., Pal, M., 2019. Preferred time headway of drivers on two-lane highways with heterogeneous traffic. *Transportation Letters* 11 (4), 200–207. URL <https://doi.org/10.1080/19427867.2017.1312859>
- Schakel, W. J., Knoop, V. L., van Arem, B., jan 2012. Integrated lane change model with relaxation and synchronization. *Transportation Research Record* 2316 (1), 47–57. URL <https://doi.org/10.3141/2316-06>
- Schakel, W. J., van Arem, B., Netten, B. D., Sep. 2010. Effects of cooperative adaptive cruise control on traffic flow stability. In: *13th International IEEE Conference on Intelligent Transportation Systems*. pp. 759–764.
- Segata, M., Dressler, F., Lo Cigno, R., Gerla, M., 2012. A simulation tool for automated platooning in mixed highway scenarios. In: *Proceedings of the 18th annual international conference on Mobile computing and networking*. ACM, pp. 389–392.
- Shen, S., Neyens, D. M., 2017. Assessing drivers’ response during automated driver support system failures with non-driving tasks. *Journal of Safety Research* 61, 149 – 155. URL <http://www.sciencedirect.com/science/article/pii/S0022437517301433>
- Shewmake, S., Jarvis, L., 2014. Hybrid cars and HOV lanes. *Transportation Research Part A: Policy and Practice* 67, 304–319.
- Shladover, S. E., Su, D., Lu, X.-Y., 2012. Impacts of cooperative adaptive cruise control on freeway traffic flow. *Transportation Research Record* 2324 (1), 63–70.
- Songchitruksa, P., Bibeka, A., Lin, L. I., Zhang, Y., et al., 2016. Incorporating driver behaviors into connected and automated vehicle simulation. Tech. rep., Center for Advancing Transportation Leadership and Safety (ATLAS Center).
- Spiliopoulou, A., Perraki, G., Papageorgiou, M., Roncoli, C., June 2017. Exploitation of acc systems towards improved traffic flow efficiency on motorways. In: *2017 5th IEEE International Conference on Models and Technologies for Intelligent Transportation Systems (MT-ITS)*. pp. 37–43.
- Talebpour, A., Mahmassani, H. S., 2016. Influence of connected and autonomous vehicles on traffic flow stability and throughput. *Transportation Research Part C: Emerging Technologies* 71, 143–163.
- Talebpour, A., Mahmassani, H. S., Bustamante, F. E., 2016. Modeling driver behavior in a connected environment: Integrated microscopic simulation of traffic and mobile wireless telecommunication systems. *Transportation Research Record* 2560 (1), 75–86. URL <https://doi.org/10.3141/2560-09>
- Transportation Research Board, 2018. *Dedicating lanes for priority or exclusive use by connected and automated vehicles*. The National Academies Press, Washington, DC. URL <https://www.nap.edu/catalog/25366>
- Treiber, M., Hennecke, A., Helbing, D., 2000. Congested traffic states in empirical observations and microscopic simulations, 1805–1824.
- Treiber, M., Kesting, A., 2013. *Traffic flow dynamics: Data, models and simulation*. Springer-Verlag Berlin Heidelberg.

- Van Arem, B., Van Driel, C. J., Visser, R., 2006. The impact of cooperative adaptive cruise control on traffic-flow characteristics. *IEEE Transactions on Intelligent Transportation Systems* 7 (4), 429–436.
- van Beinum, A., Farah, H., Wegman, F., Hoogendoorn, S., 2018. Driving behaviour at motorway ramps and weaving segments based on empirical trajectory data. *Transportation Research Part C: Emerging Technologies* 92, 426 – 441.
URL <http://www.sciencedirect.com/science/article/pii/S0968090X18305928>
- Wang, H., Qin, Y., Wang, W., Chen, J., 2019a. Stability of CACC-manual heterogeneous vehicular flow with partial CACC performance degrading. *Transportmetrica B: Transport Dynamics* 7 (1), 788–813.
URL <https://doi.org/10.1080/21680566.2018.1517058>
- Wang, M., van Maarseveen, S., Happee, R., Tool, O., van Arem, B., 2019b. Benefits and risks of truck platooning on freeway operations near entrance ramp. *Transportation Research Record* 2673 (8), 588–602.
URL <https://doi.org/10.1177/0361198119842821>
- Wang, R., Li, Y., Work, D. B., 2017a. Comparing traffic state estimators for mixed human and automated traffic flows. *Transportation Research Part C: Emerging Technologies* 78, 95 – 110.
URL <http://www.sciencedirect.com/science/article/pii/S0968090X17300517>
- Wang, Z., Wu, G., Hao, P., Boriboonsomsin, K., Barth, M., 2017b. Developing a platoon-wide eco-cooperative adaptive cruise control (CACC) system. In: 2017 IEEE Intelligent Vehicles Symposium (IV). IEEE, pp. 1256–1261.
- Wiedemann, R., 1974. Simulation des Straenverkehrsflusses. Ph.D. thesis, Karlsruhe.
- Wiedemann, R., 1991. Modelling of rti-elements on multi-lane roads. In: Drive Conference (1991: Brussels, Belgium). Vol. 2.
- Xiao, L., Wang, M., Schakel, W., van Arem, B., 2018. Unravelling effects of cooperative adaptive cruise control deactivation on traffic flow characteristics at merging bottlenecks. *Transportation Research Part C: Emerging Technologies* 96, 380 – 397.
URL <http://www.sciencedirect.com/science/article/pii/S0968090X1830528X>
- Xu, S., Peng, H., 2019. Design, analysis, and experiments of preview path tracking control for autonomous vehicles. *IEEE Transactions on Intelligent Transportation Systems*, 1–11.
- Young, I. T., 1977. Proof without prejudice: use of the Kolmogorov-Smirnov test for the analysis of histograms from flow systems and other sources. *Journal of Histochemistry & Cytochemistry* 25 (7), 935–941.
- Zhang, X., Ma, J., Smith, B., Liu, J., 2018. Operational performance evaluation of the managed lane strategy for early deployment of cooperative adaptive cruise control. Tech. rep.
- Zhao, W., Ngoduy, D., Shepherd, S., Liu, R., Papageorgiou, M., 2018. A platoon based cooperative eco-driving model for mixed automated and human-driven vehicles at a signalised intersection. *Transportation Research Part C: Emerging Technologies* 95, 802 – 821.
URL <http://www.sciencedirect.com/science/article/pii/S0968090X18307423>
- Zhong, Z., 2018. Assessing the effectiveness of managed lane strategies for the rapid deployment of cooperative adaptive cruise control technology. Ph.D. thesis, New Jersey Institute of Technology.
- Zhong, Z., Joyoung, L., Zhao, L., 2017. Evaluations of Managed Lane Strategies for Arterial Deployment of Cooperative Adaptive Cruise Control. In: 96th Transportation Research Board Annual Meeting. Washington DC, USA.
- Zhong, Z., Lee, J., 2019. The effectiveness of managed lane strategies for the near-term deployment of cooperative adaptive cruise control. *Transportation Research Part A: Policy and Practice* 129, 257 – 270.
URL <http://www.sciencedirect.com/science/article/pii/S0965856419303520>